

## Fabrication of PES MMMs with Improved Separation Performances Using Two-Dimensional rGO/ZIF-8 and MoS<sub>2</sub>/ZIF-8 Nanofillers

Noor Fauziyah Ishak<sup>1\*</sup>, Nur Hidayati Othman<sup>1</sup>, Najihah Jamil<sup>1</sup>, Nur Hashimah Alias<sup>1</sup>, Fauziah Marpani<sup>1</sup>, Munawar Zaman Shahrudin<sup>1</sup>, Lau Woei Jye<sup>2</sup> and Ahmad Fauzi Ismail<sup>2</sup>

<sup>1</sup>School of Chemical Engineering, College of Engineering, Universiti Teknologi MARA, 40450 UiTM, Shah Alam, Selangor, Malaysia

<sup>2</sup>Advanced Membrane Technology Research Centre (AMTEC), Universiti Teknologi Malaysia, 81310 UTM, Skudai, Johor, Malaysia

### ABSTRACT

Modifying polymeric membranes using nanofiller is a promising method to enhance gas permeability and selectivity performance. This work used two types of ZIF-8 functionalized-2D nanofillers to fabricate polyethersulfone mixed matrix membranes. The rGO/ZIF-8 and MoS<sub>2</sub>/ZIF-8 nanofillers were first synthesised and characterised using FTIR and XRD. Then, 10 wt% of each nanofillers was added to the PES solution. TGA analysis indicates that MMMs containing rGO/ZIF-8 and MoS<sub>2</sub>/ZIF-8 exhibit improved thermal stability. No additional peaks in FTIR and XRD were observed in the MMMs, indicating that the 2D nanofillers were compatible with the PES matrix. The MMMs show significantly enhanced gas separation properties where the highest selectivity was observed for 10 wt%PRG/Pebax membrane of 35.71 with CO<sub>2</sub> permeability of 611 barrer and CH<sub>4</sub> permeability of 17.11 barrer. These results confirm the possibility of using 2D nanofillers to develop high-performance membranes for gas separation.

### ARTICLE INFO

#### Article history:

Received: 07 September 2022

Accepted: 25 January 2023

Published: 21 July 2023

DOI: <https://doi.org/10.47836/pjst.31.5.23>

#### E-mail addresses:

noorfauziyah@uitm.edu.my (Noor Fauziyah Ishak)

nurhidayati0955@uitm.edu.my (Nur Hidayati Othman)

najihah\_jamil90@yahoo.com (Najihah Jamil)

nurhashimah@uitm.edu.my (Nur Hashimah Alias)

fauziah176@uitm.edu.my (Fauziah Marpani)

munawar\_zaman@salam.uitm.edu.my

(Munawar Zaman Shahrudin)

lwoejjye@utm.my (Lau Woei Jye)

afauzi@utm.my; fauzi.ismail@gmail.com (Ahmad Fauzi Ismail)

\*Corresponding author

*Keywords:* 2D nanofillers, gas separation, mixed matrix membranes, MoS<sub>2</sub>, rGO, ZIF-8

### INTRODUCTION

Gas separation is extensively used in carbon capture and storage, air purification, natural gas upgrading and hydrogen recovery. The

conservative method such as cryogenic distillation, adsorption and absorption are not economically satisfied due to the high heat and energy consumption. Membrane technology, which does not need any heat, does not utilise any chemicals, has no emissions, has a smaller footprint and a simple setup, is considered a competitive technology for gas separation. Membrane separation for an ideal gas must be high permeability and selectivity to the desired gases. However, the membrane is known to be subjected to a trade-off between selectivity and permeability (Jamil et al., 2019). Achieving high gas permeation and excellent selectivity is still a big challenge today. The tremendous development of mixed matrix membranes (MMMs) for gas separation was recently discovered by academics (Kamble et al., 2021). The MMMs consist of organic-inorganic hybrid membranes, which are polymeric as substrate membranes and are incorporated with inorganic materials as filler. In this regard, inorganic filler as a two-dimensional (2D) material is extensively used in MMMs fabrication.

The developing 2D layered materials of atomic thickness have provided an extraordinary opportunity to improve high-performance membrane materials with unique nanopores and/or nanochannels (Liu et al., 2016). Graphene and its derivatives are of specific attention for molecular separation (Dong et al., 2016). However, there are many other 2D nanomaterials, such as metal-organic framework (MOF), transition metal dichalcogenide (TMD), hexagonal boron nitride (h-BN) and molybdenum disulphide ( $\text{MoS}_2$ ), which possess unique and intriguing structural features suitable for membrane application that have not been widely studied. Besides material properties, these 2D materials can be massively produced using high-yield and scalable liquid-based exfoliation methods. The 2D nanosheets, single-layered or few-layered, can be stacked in parallel to form sub-nanometre channels between the sheets. Such laminate membranes usually possess exceptional molecular-sieving properties as gas transport resistance is minimised and thus maximises gas flux (Moghadam & Park, 2019).

Due to molecular-sieving properties that allow mitigation of recognised participation phenomenon in polymer membranes by strongly interacting with the polymer chains, these 2D nanosheets are preferably utilised as nanofillers. Therefore, enormous effort has been devoted to implementing zeolitic imidazolate frameworks-8 (ZIF-8) as one of the capable inorganic MOFs to enhance materials compatibility in MMMs fabrication (Amedi & Aghajani, 2017; Jusoh et al., 2016; Mei et al., 2020). For instance, Hadi et al. (2021) used 10 wt% of ZIF-8 to fabricate hollow fibre MMMs, resulting in improved  $\text{O}_2/\text{N}_2$  gas separation with ideal selectivity of 5.25 (Hadi et al., 2021). However, excessive ZIF-8 loading in the MMMs fabrication would occur defects due to agglomeration phenomena. Recently, it has been a major challenge to prepare defect-free MMMs that implement ZIF-8 as a nanofiller.

Thus, this work aims to develop a new type of MMMs by functionalised ZIF-8 with other materials, which are reduced graphene oxide (rGO) and MoS<sub>2</sub> as potential 2D nanofillers. These two materials incorporated with ZIF-8 are promising as emerging 2D nanomaterials that improve gas permeability and selectivity.

## MATERIALS AND METHODS

### Materials

Graphite powders (MW = 12.01 g/mol), N-methyl-2-pyrrolidone (NMP, 99% purity), polyethylene glycol (PEG, MW = 400), hydrogen peroxide (H<sub>2</sub>O<sub>2</sub>, 30 wt%), and hydrochloric acid (HCl, 37% purity) were purchased at Merck Sdn. Bhd., Malaysia. Meanwhile, concentrated sulphuric acid (H<sub>2</sub>SO<sub>4</sub>, 95–98% purity) and potassium permanganate (KMnO<sub>4</sub>, MW = 158.05 g/mol) was purchased at R&M Chemicals. Zinc nitrate hexahydrate (Zn(NO<sub>3</sub>)<sub>2</sub>·6H<sub>2</sub>O, MW = 297.49 g/mol) and 2-methylimidazole (H-MeIM, MW = 82.10 g/mol) and polyethersulfone (PES) were purchased at Sigma-Aldrich (M) Sdn. Bhd., Malaysia. Sodium nitrate (NaNO<sub>3</sub>, MW = 84.99 g/mol), L(+) ascorbic acid (C<sub>6</sub>H<sub>8</sub>O<sub>6</sub>, MW = 176.13 g/mol) and methylalcohol (MeOH, MW = 32.04 g/mol) were purchased at SYSTERM. Poly (ether block amide) (PEBAX-1657) was used as a coating material to form a selective membrane layer purchased at Arkema.

### Preparation of rGO/ZIF-8 and MoS<sub>2</sub>/ZIF-8 Nanofillers

Graphene oxide (GO) and reduced graphene oxide (rGO) was synthesised by using combined chemical and mechanical method (Zainuddin et al., 2017). Firstly, GO was prepared using Hummer's method, where 5 g of graphite powder was mixed with 200 ml of H<sub>2</sub>SO<sub>4</sub> and 30 g of KMnO<sub>4</sub>. Then, 30 ml of H<sub>2</sub>O<sub>2</sub> was used to stop the reaction and washed with HCl and distilled water to adjust pH to get neutral GO. The GO was deoxygenation using C<sub>6</sub>H<sub>8</sub>O<sub>6</sub> as a reducing agent to produce rGO suspension. Meanwhile, template growth of ZIF-8 was used to synthesise rGO/ZIF-8 nanofillers by stirring 4.8 g of Zn(NO<sub>3</sub>)<sub>2</sub>·6H<sub>2</sub>O and 10.6 g of 2-Hmim in 180.8 ml of methanol for 1 hr. 70 mg of rGO suspension was immersed in the Zn(NO<sub>3</sub>)<sub>2</sub> methanol solution and added into the previous Zn(NO<sub>3</sub>)<sub>2</sub> solution. This solution was continued stirring for 8 hr and then ultrasonic for another 1 hr. Its precipitate was collected by washing with third times of 50 ml of methanol to remove the leftover precursor. The last step was to dry the rGO/ZIF-8 nanofillers for 4 hr at 60°C under vacuum conditions. All these steps were repeated for synthesising MoS<sub>2</sub>-ZIF/8 nanofiller using MoS<sub>2</sub> powder to replace rGO suspension.

### Preparation of rGO/ZIF-8 and MoS<sub>2</sub>/ZIF-8 PES MMMs

PES as a based membrane was first prepared by blending with NMP as a solvent to get a dope solution. Then 10 wt% of rGO/ZIF-8 and 10 wt% MoS<sub>2</sub>-ZIF/8 nanofillers were

added into the dope solution of PES-NMP to prepare rGO/ZIF-8 and MoS<sub>2</sub>/ZIF-8 PES MMMs solution, respectively. Both prepared dope solutions were sonicated and degassed for 1 hr, then cast onto a glass plate using a casting knife at a gap of 200 μm. The casted MMM sheets were immersed immediately in the coagulation bath for 24 hr using the phase inversion technique, followed by a second immersion in another coagulation bath to remove any residual before being air-dried (Akhair et al., 2017; Jamil et al., 2019). A bare PES membrane was also prepared for the comparison study without adding a nanofiller.

### Preparation of Coated rGO/ZIF-8 and MoS<sub>2</sub>/ZIF-8 PES MMMs

Pebax solution with 3 wt% concentration was prepared by dissolving 3 g of Pebax 1657 pellet in a 70/30 ethanol/water ratio. The solution was then heated at 60°C and stirred for 1 hr to achieve a homogenous solution before being cool down at room temperature. Prior to dip-coating, the Pebax solution was sonicated for 30 min. The coating process was repeated 3 times at 60s intervals. After each coating step, the membranes were dried at 60°C for 25 min to allow solvent vaporisation. Table 1 was summarised the list of abbreviations for each of the membranes coated with Pebax.

Table 1

*List of abbreviations for membranes coated with 3 wt% of Pebax*

Sample	List of abbreviations
Bare PES/Pebax	PB/Pebax
10 rGO/ZIF-8PES/Pebax	10 wt% PRG/Pebax
10 MOS <sub>2</sub> /ZIF-8PES/Pebax	10 wt% PMZ/Pebax

### Characterisation and Gas Permeation Testing

The synthesised nanofillers and fabricated MMMs were characterised using XRD (PANalytical, X'Pert Pro), FTIR (Perkin Elmer, Spectrum One) and TGA (Mettler Toledo, TGA/SDTA 851E) analysis. Then, the morphology was observed by scanning electron microscopy (SEM) (Hitachi Backs Catter Detector S-3000). An in-house 316 stainless steel gas permeation cell was used for the gas permeation testing with an effective area of 22.9 cm<sup>2</sup> at constant volume, but variable pressure was applied. The prepared MMMs were cut into desired circular shapes, and two gases were used for this method which is CO<sub>2</sub> (3.30 Å) and CH<sub>4</sub> (3.80 Å), with high purity of 99.99%. During the testing, a bubble flow meter was used to measure the permeation rate of these gas streams and repeated 3 times to get an average value. The gas permeability was determined from the following Equation 1:

$$P = \frac{Q \times L}{A \times \Delta P} \quad (1)$$

where  $Q$  and  $L$  are permeating volumetric flowrate (mol/s) and membrane thickness (m), respectively. Meanwhile,  $A$  is the effective membrane area, and  $\Delta P$  is the pressure difference. Thus, the selectivity performance for gas I to gas j was calculated using Equation 2, as reported by (Jamil et al., 2019):

$$Selectivity = \frac{P_i}{P_j} \quad (2)$$

where the  $P_i$  and  $P_j$  are permeability values for gas i and j, respectively.

## RESULTS AND DISCUSSION

### XRD Analysis

Figure 1 illustrates the XRD of nanofillers and MMMs. It can be seen that a weak MoS<sub>2</sub> peak appears at 103, confirming that a successful intercalation of ZIF-8 into MoS<sub>2</sub> can be obtained through the sonication process. Besides that, the exfoliated MoS<sub>2</sub> planes in MoS<sub>2</sub>/ZIF-8 were observed to shift to a slightly lower angle from  $2\theta=39.45^\circ$  to  $2\theta=39.01^\circ$  which is attributed to the increase of interlayer spacing of MoS<sub>2</sub> due to intercalation of ZIF-8 into MoS<sub>2</sub> layers (Gao et al., 2013; Ries et al., 2019). The XRD pattern for rGO/ZIF-8 was almost similar to a single ZIF-8. It indicates that the in-situ functionalization of ZIF-8 into rGO does not alter their intrinsic properties, or the amount of MoS<sub>2</sub> and rGO added was too small to reach the detection limit. Both nanofillers had sharper peaks compared to a single ZIF-8, indicating that the nanofillers' crystallite size was larger than ZIF-8 (Lai et al., 2016).

The XRD patterns of PB/Pebax and PES MMMs/Pebax incorporated with 10 wt% of PRG and PMZ were then compared. It was observed that the amorphous phase of the PES polymer dominated the XRD patterns of MMMs. No significant changes in the XRD pattern of 10PRG/Pebax indicate that the amount of rGO/ZIF-8 nanofillers added into the polymer matrix is quite low to affect the structure of PES. Interestingly, for 10PMZ/Pebax membranes, a weak peak of MoS<sub>2</sub> at  $2\theta=10.82^\circ$ , which is related to (002) planes, appeared, which designates that the amount of MoS<sub>2</sub>/ZIF-8 is high enough for well-preserved the MoS<sub>2</sub> crystallite structure even after incorporation of them into the amorphous polymer structure.

### FTIR Analysis

Figure 2 shows the functional group peaks obtained through FTIR analysis. The FTIR analysis of ZIF-8 shows spectra that are associated with C=N stretching ( $1596\text{ cm}^{-1}$ ), vibration from entire ring stretching ( $1434\text{--}1312\text{ cm}^{-1}$ ) and C-N stretching ( $1150\text{ cm}^{-1}$ ). The peaks at  $994\text{ cm}^{-1}$  and  $750\text{ cm}^{-1}$  could also correspond to the in-plane C-N bending vibration and C-H bending mode (Feng et al., 2016), respectively. At band  $690\text{ cm}^{-1}$ , the

ring out-of-plane bending vibration of Hmim was observed. Similarly, the very small peak was observed at a higher wavenumber ( $3450\text{ cm}^{-1}$ ), which might be attributed to the N-H stretching vibration from residual Hmim. For rGO/ZIF-8, it can be observed that several major peaks of ZIF-8 spectra are retained, indicating that the in-situ functionalisation of rGO does not interrupt the coordination of 2-methylimidazole linker to the zinc(II) centres and thus the formation of ZIF-8 (Wang et al., 2017). For MoS<sub>2</sub>/ZIF-8, the broad absorption band at  $1748\text{ cm}^{-1}$  and  $3541\text{ cm}^{-1}$  belongs to the carbonyl stretching vibrations (Kumar et al., 2016), and O-H stretching can be seen. Additional peaks at  $1232\text{ cm}^{-1}$  belonging to epoxy C-O-C were also observed.

PB/Pebax spectra band shows spectra band at  $1110\text{ cm}^{-1}$  and  $1745\text{ cm}^{-1}$  recognised as C-O-C and -C=O stretching vibrations, respectively. Two other bands, also observed at  $1640$  and  $3309\text{ m}^{-1}$ , are attributed to the existence of H-N-C=O and N-H groups in the hard polyamide (PA) segment, respectively (Cheshomi et al., 2018). The PES characteristic peaks consist of a benzene ring ( $2952\text{ cm}^{-1}$ ), an ether bond, and a sulphone structure ( $1050\text{ cm}^{-1}$ ) (Qu et al., 2010) that appeared in the spectra, although generally, the characteristic peak of Pebax is more prominent compared to PES, MoS<sub>2</sub>/ZIF-8 and rGO/ZIF-8 nanofillers that were

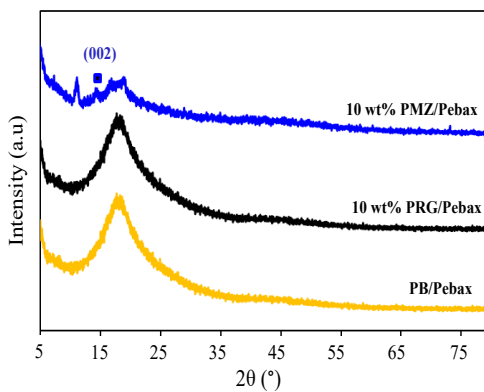
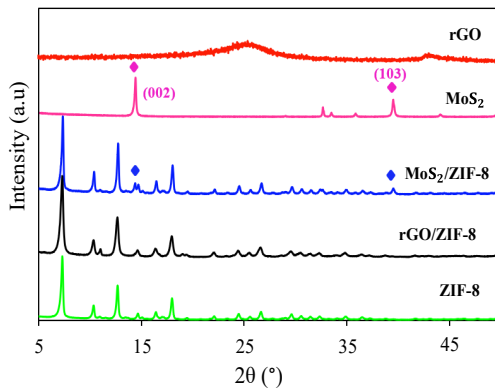


Figure 1. XRD pattern of nanofillers and MMMs

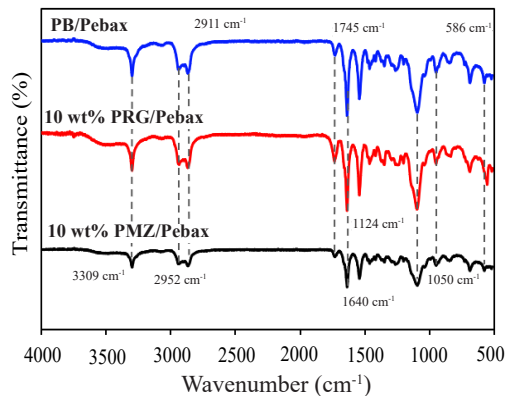
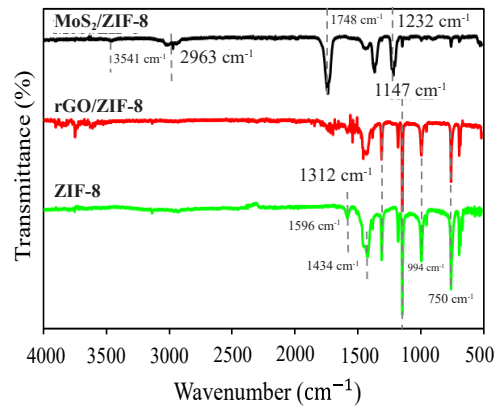


Figure 2. FTIR spectra of nanofillers and MMMs

incorporated inside the membrane. It might be due to the presence of polar pendant groups such as ethylene oxide in Pebax, where the more polar the molecule, the stronger the size of the IR spectrum.

### TGA Analysis

Thermal degradation analysis is important to analyse thermal stability for materials application. Figure 3 shows the TGA analysis of nanofillers and MMMs. Single component MoS<sub>2</sub> and rGO are the most stable materials compared to ZIF-8. ZIF-8 is quite stable and possesses little weight loss below 350°C. However, at a temperature range of 600-800°C, it was observed that 55% of weight loss was occurred. This phenomenon indicated that ZIF-8 was converted into zinc oxide as in the thermal decomposition process (L. Dong et al., 2016). As a result, it can be observed that once rGO and MoS<sub>2</sub> were functionalised with ZIF-8, the thermal stability of the hybrid nanofillers was increased.

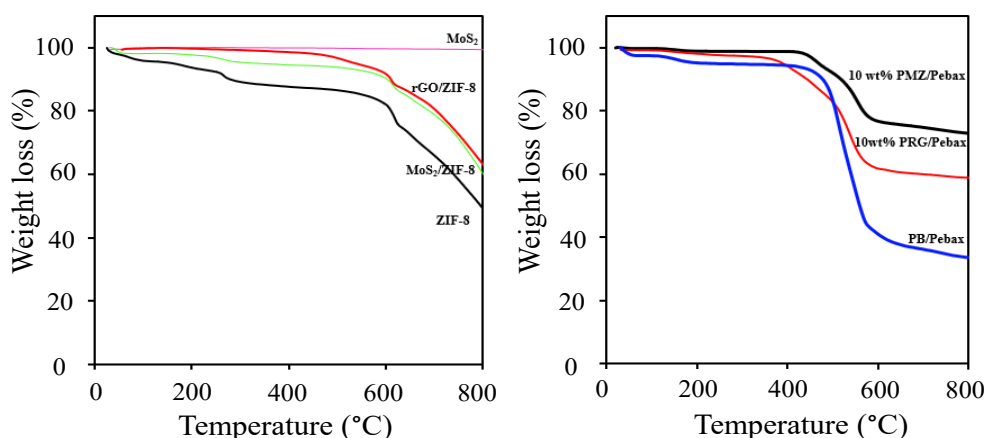


Figure 3. TGA of nanofillers and MMMs

Meanwhile, for PB/Pebax and both MMMs, there are three degradation steps, i.e. the first step is due to the removal of residual solvent and possibly adsorbed water (< 200°C), the second step is due to major polymer chain carbonisation (< 480°C) and finally the degradation of the polymer chain (> 480°C). Overall, the total weight loss for both MMMs with nanofillers was significantly lower than the PB/Pebax membrane, in which 10 wt%PMZ/Pebax membrane exhibited the most thermal stability of the total weight loss was less than 30%.

## SEM Analysis

The cross-section SEM structure of the selective layer for Pebax coated on the PES and PES MMMs is presented in Figure 4. Overall, the SEM structures show that the selective layers of Pebax were uniformly coated with thicknesses of around 0.5-0.8  $\mu\text{m}$  and 1.2  $\mu\text{m}$  for MMMs and bare membrane, respectively. The selective layer of MMMs was thinner than bare PES (PB/Pebax). Besides that, it was noted that both MMMs exhibited straighter and more organised finger form structures than PB/Pebax due to the addition of nanofillers in MMMs fabrication. Thus, these two nanofillers were contributed in better interaction with pebax layer by forming higher adhesion force with thinner coating layer (Garcia-Fayos et al., 2018). The coating thickness of MMMs was in a good range due to higher gas permeability being performed at less selective layer thickness.

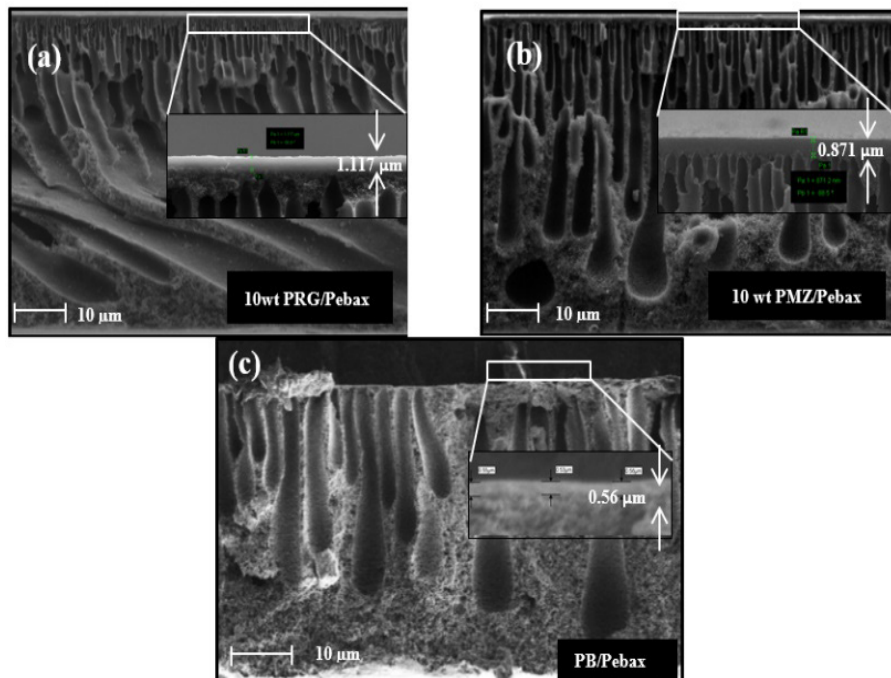


Figure 4. SEM of MMMs

## Gas Permeation Measurement

The  $\text{CO}_2$  and  $\text{CH}_4$  gas permeabilities and their selectivity are presented in Figure 5. In general, the permeability for both gases increases with increased operating pressure. However, it was noted that at a high operating pressure of 5 bar, particularly for bare PES membrane (PB/Pebax),  $\text{CH}_4$  permeability decreased, leading to lower  $\text{CO}_2/\text{CH}_4$  selectivity compared to the low operating pressure of 1 bar. This trend occurred due to the polymer



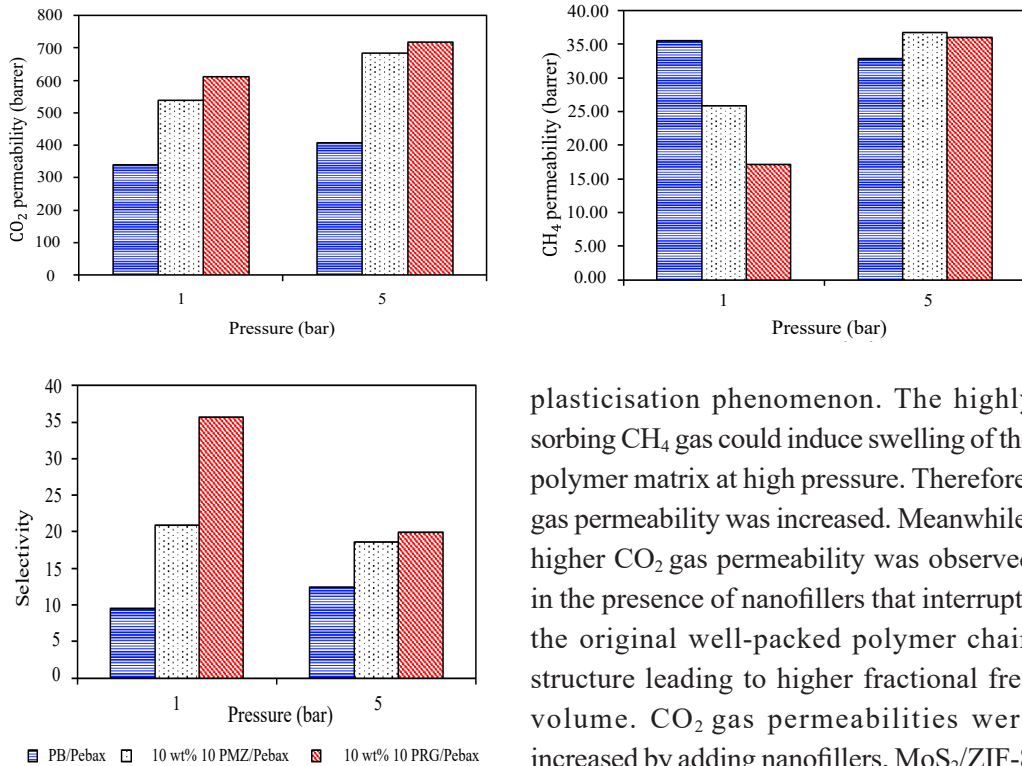


Figure 5. Permeabilities and selectivity of PB/Pebax, 10 wt% PMZ/Pebax and 10 wt% PRG/Pebax

plasticisation phenomenon. The highly sorbing CH<sub>4</sub> gas could induce swelling of the polymer matrix at high pressure. Therefore, gas permeability was increased. Meanwhile, higher CO<sub>2</sub> gas permeability was observed in the presence of nanofillers that interrupts the original well-packed polymer chain structure leading to higher fractional free volume. CO<sub>2</sub> gas permeabilities were increased by adding nanofillers, MoS<sub>2</sub>/ZIF-8 and rGO/zif-8, for 10 wt% PMZ/Pebax and 10 wt% PRG/Pebax, respectively. Thus, the CO<sub>2</sub>/CH<sub>4</sub> selectivities for these two MMMs

were higher at low operating pressure compared to high operating pressure. The highest selectivity of 35.71 was observed for 10 wt%PRG/Pebax membrane with CO<sub>2</sub> permeability of 611 barrer and CH<sub>4</sub> permeability of 17.11 barrer.

Meanwhile, Table 2 was illustrated for gas permeability and selectivity of MMMs with different polymers and nanofillers from the literature to compare with this work. From the literature, more studies were found to use ZIF-8 as a single nanofiller, improving gas

Table 2  
Gas permeability and selectivity of MMMs with different polymers and nanofillers

Polymer	Nanofiller	Operating Pressure	CO <sub>2</sub> permeability	Selectivity	Reference
6FDA-durene polymer	10 wt% of ZIF-8	1 bar	1426.75 Barrer	CO <sub>2</sub> /CH <sub>4</sub> selectivity of 28.70	Jusoh et al. (2016)

Table 2 (Continue)

Polymer	Nanofiller	Operating Pressure	CO <sub>2</sub> permeability	Selectivity	Reference
Polysulfone (Psf)	0.15 wt% of MoS <sub>2</sub>	2 bar	64 Barrer	CO <sub>2</sub> /N <sub>2</sub> selectivity of 93	Shen et al. (2016)
Polyvinylidene Fluoride (PVDF)	0.5 wt% of GO	5 bar	0.897 Barrer	CO <sub>2</sub> /CH <sub>4</sub> selectivity of 40.63	Feijani et al. (2018)
Polysulfone (Psf)	0.5 wt% of aminated rGO	4 bar	65.20 Barrer	CO <sub>2</sub> /CH <sub>4</sub> selectivity of 14.82	Krishnan et al. (2020)
Polysulfone (Psf)	10 wt% of ZIF-8	4 bar	36.60 Barrer	CO <sub>2</sub> /CH <sub>4</sub> selectivity of 27.72	Mei et al. (2020)
Polysulfone (Psf)	0.25 wt% of GO	1 bar	35.42 Barrer	CO <sub>2</sub> /CH <sub>4</sub> selectivity of 6.42	Sainath et al. (2021)
Polyethersulfone (PES)	10 wt% of rGO/ZIF-8	1 bar	611 Barrer	CO <sub>2</sub> /CH <sub>4</sub> selectivity of 35.71	This work
		5 bar	725 Barrer	CO <sub>2</sub> /CH <sub>4</sub> selectivity of 20.14	
Polyethersulfone (PES)	10 wt% of MoS <sub>2</sub> /ZIF-8	1 bar	551 Barrer	CO <sub>2</sub> /CH <sub>4</sub> selectivity of 21.67	This work
		5 bar	682 Barrer	CO <sub>2</sub> /CH <sub>4</sub> selectivity of 19.86	

permeability and selectivity. Mei et al. (2020) reported that 10 wt% of ZIF-8 was used in Psf MMM fabrication to establish CO<sub>2</sub> permeability of 36.60 Barrer with CO<sub>2</sub>/CH<sub>4</sub> selectivity of 27.72 at an operating pressure of 4 bar. In addition, Krishnan et al. (2020) added 0.5 wt% of aminated rGO in Psf MMM fabrication, resulting in CO<sub>2</sub> permeability of 65.20 Barrer with CO<sub>2</sub>/CH<sub>4</sub> selectivity of 14.82 at an operating pressure of 4 bar. In

this regard, the present study functionalised ZIF-8 with two different materials, rGO and MoS<sub>2</sub> to implement as nanofillers in PES MMMs fabrication. Therefore, both nanofillers have successfully enhanced the performance of gas permeability and selectivity at two different operating pressure (Table 2).

## CONCLUSION

The demand for cost-efficient separation necessitates membranes with high gas permeability and excellent selectivity, providing the pathway for the further development of membrane materials. In this study, ZIF-8 was successfully functionalised with two different 2D materials, i.e., rGO and MoS<sub>2</sub> and further incorporated into the PES matrix to form MMMs. The results indicate that the 2D nanofillers can significantly increase the gas permeability, especially CO<sub>2</sub> while maintaining high selectivity. These nanofillers could also minimise the plasticisation effects of the membrane, especially at high operating pressure. It is due to the laminate structure of 2D materials, which minimises gas transport resistance and consequently maximises gas permeability.

## ACKNOWLEDGEMENTS

The authors acknowledged the Ministry of Higher Education (MOHE) and Universiti Teknologi Mara (UiTM), Malaysia for the financial support via the FRGS grant, 600-IRMI/FRGS 5/3 (087/2017). Nur Hidayati Othman would also like to thank Professor Nalan Kabay (Ege Üniversitesi) and The Scientific and Technological Research Council of Turkey (TÜBİTAK) for 2221-Fellowship for Visiting Scientists and Scientists on Sabbatical Leave (Short-term).

## REFERENCES

- Akhaier, S. S. M., Harun, Z., Jamalludin, M. R., Shuhor, M. F., Kamarudin, N. H., Yunos, M. Z., Ahmad, A., & Azhar, M. F. H. (2017). Polymer mixed matrix membrane with graphene oxide for humic acid performances. *Chemical Engineering Transactions*, 56, 697-702. <https://doi.org/10.3303/CET1756117>
- Amedi, H. R., & Aghajani, M. (2017). Aminosilane-functionalized ZIF-8/PEBA mixed matrix membrane for gas separation application. *Microporous and Mesoporous Materials*, 247, 124-135. <https://doi.org/10.1016/j.micromeso.2017.04.001>
- Cheshomi, N., Pakizeh, M., & Namvar-Mahboub, M. (2018). Preparation and characterization of TiO<sub>2</sub>/Pebax/ (PSf-PES) thin film nanocomposite membrane for humic acid removal from water. *Polymers for Advanced Technologies*, 29(4), 1303-1312. <https://doi.org/10.1002/pat.4242>
- Dong, G., Hou, J., Wang, J., Zhang, Y., Chen, V., & Liu, J. (2016). Enhanced CO<sub>2</sub>/N<sub>2</sub> separation by porous reduced graphene oxide/Pebax mixed matrix membranes. *Journal of Membrane Science*, 520, 860-868. <https://doi.org/10.1016/j.memsci.2016.08.059>

- Dong, L., Chen, M., Li, J., Shi, D., Dong, W., Li, X., & Bai, Y. (2016). Metal-organic framework-graphene oxide composites: A facile method to highly improve the CO<sub>2</sub> separation performance of mixed matrix membranes. *Journal of Membrane Science*, 520, 801-811. doi: <https://doi.org/10.1016/j.memsci.2016.08.043>
- Feijani, E. A., Tavassoli, A., Mahdavi, H., & Molavi, H. (2018). Effective gas separation through graphene oxide containing mixed matrix membranes. *Journal of Applied Polymer Science*, 135, Article 46271. <https://doi.org/10.1002/app.46271>
- Feng, Y., Li, Y., Xu, M., Liu, S., & Yao, J. (2016). Fast adsorption of methyl blue on zeolitic imidazolate framework-8 and its adsorption mechanism. *RSC Advances*, 6(111), 109608-109612. <https://doi.org/10.1039/C6RA23870J>
- Gao, D., Si, M., Li, J., Zhang, J., Zhang, Z., Yang, Z., & Xue, D. (2013). Ferromagnetism in freestanding MoS<sub>2</sub> nanosheets. *Nanoscale Research Letters*, 8(1), 1-8. <https://doi.org/10.1186/1556-276X-8-129>
- Garcia-Fayos, J., Balaguer, M., Baumann, S., & Serra, J. M. (2018). Dual-phase membrane based on LaCo<sub>0.2</sub>Ni<sub>0.4</sub>Fe<sub>0.4</sub>O<sub>3-x</sub>Ce<sub>0.8</sub>Gd<sub>0.2</sub>O<sub>2-x</sub> composition for oxygen permeation under CO<sub>2</sub>/SO<sub>2</sub>-rich gas environments. *Journal of Membrane Science*, 548, 117-124. doi: <https://doi.org/10.1016/j.memsci.2017.11.006>
- Hadi, A., Karimi-Sabet, J., Nikkho, S., & Dastbaz, A. (2021). Fabrication of ZIF-8/polyethersulfone (PES) mixed matrix hollow fiber membranes for O<sub>2</sub>/N<sub>2</sub> separation. *Chemical Papers*, 75, 4129-4145. <https://doi.org/10.1007/s11696-021-01642-7>
- Jamil, N., Othman, N. H., Alias, N. H., Shahrudin, M. Z., Roslan, R. A., Lau, W. J., & Ismail, A. F. (2019). Mixed matrix membranes incorporated with reduced graphene oxide (rGO) and zeolitic imidazole framework-8 (ZIF-8) nanofillers for gas separation. *Journal of Solid State Chemistry*, 270, 419-427. <https://doi.org/10.1016/j.jssc.2018.11.028>
- Jusoh, N., Yeong, Y. F., Lau, K. K., & Shariff, A. M. (2016). Mixed matrix membranes comprising of ZIF-8 nanofillers for enhanced gas transport properties. *Procedia Engineering*, 148, 1259-1265. <https://doi.org/10.1016/j.proeng.2016.06.499>
- Kamble, A. R., Patel, C. M., & Murthy, Z. V. P. (2021). A review on the recent advances in mixed matrix membranes for gas separation processes. *Renewable and Sustainable Energy Reviews*, 145, Article 111062. <https://doi.org/10.1016/j.rser.2021.111062>
- Krishnan, G., Mohtar, S. S., Aziz, F., Jaafar, J., Yusof, N., Salleh, W. N. W., & Ismail, A. F. (2020). Mixed matrix composite membranes based on amination of reduced graphene oxide for CO<sub>2</sub> separation: Effects of heating time and nanofiller loading. *Korean Journal of Chemical Engineering*, 37(12), 2287-2294. <https://doi.org/10.1007/s11814-020-0649-4>
- Kumar, S., Sharma, V., Bhattacharyya, K., & Krishnan, V. (2016). Synergetic effect of MoS<sub>2</sub>-RGO doping to enhance the photocatalytic performance of ZnO nanoparticles. *New Journal of Chemistry*, 40(6), 5185-5197. <https://doi.org/10.1039/C5NJ03595C>
- Lai, L. S., Yeong, Y. F., Lau, K. K., & Shariff, A. M. (2016). Effect of synthesis parameters on the formation of ZIF-8 under microwave-assisted solvothermal. *Procedia Engineering*, 148, 35-42. <https://doi.org/10.1016/j.proeng.2016.06.481>

- Liu, G., Jin, W., & Xu, N. (2016). Two-dimensional-material membranes: A new family of high-performance separation membranes. *Angewandte Chemie International Edition*, 55(43), 13384-13397. <https://doi.org/10.1002/anie.201600438>
- Mei, X., Yang, S., Lu, P., Zhang, Y., & Zhang, J. (2020). Improving the selectivity of ZIF-8/Polysulfone-Mixed Matrix Membranes by Polydopamine Modification for H<sub>2</sub>/CO<sub>2</sub> separation. *Frontiers in Chemistry*, 8, Article 528. <https://doi.org/10.3389/fchem.2020.00528>
- Moghadam, F., & Park, H. B. (2019). 2D nanoporous materials: Membrane platform for gas and liquid separations. *2D Materials*, 6(4), Article 042002. <https://doi.org/10.1088/2053-1583/ab1519>
- Qu, P., Tang, H., Gao, Y., Zhang, L., & Wang, S. (2010). Polyethersulfone composite membrane blended with cellulose fibrils. *BioResources*, 5(4), 2323-2336.
- Ries, L., Petit, E., Michel, T., Diogo, C. C., Gervais, C., Salameh, C., Bechelany, M., Balme, S., Miele, P., Onofrio, N., & Voiry, D. (2019). Enhanced sieving from exfoliated MoS<sub>2</sub> membranes via covalent functionalization. *Nature Materials*, 18(10), 1112-1117. <https://doi.org/10.1038/s41563-019-0464-7>
- Sainath, K., Modi, A., & Bellare, J. (2021). CO<sub>2</sub>/CH<sub>4</sub> mixed gas separation using graphene oxide nanosheets embedded hollow fiber membranes: Evaluating effect of filler concentration on performance. *Chemical Engineering Journal Advances*, 5, Article 100074. <https://doi.org/10.1016/j.cej.2020.100074>
- Shen, Y., Wang, H., Zhang, X., & Zhang, Y. (2016). MoS<sub>2</sub> nanosheets functionalized composite mixed matrix membrane for enhanced CO<sub>2</sub> capture via surface drop-coating method. *ACS Applied Materials & Interfaces*, 8(35), 23371-23378. <https://doi.org/10.1021/acsami.6b07153>
- Wang, H., Wang, Y., Jia, A., Wang, C., Wu, L., Yang, Y., & Wang, Y. (2017). A novel bifunctional Pd-ZIF-8/rGO catalyst with spatially separated active sites for the tandem Knoevenagel condensation-reduction reaction. *Catalysis Science & Technology*, 7(23), 5572-5584. <https://doi.org/10.1039/C7CY01725A>
- Zainuddin, M., F., Raikhan, N. N. H., Othman, N. H., & Abdullah, W. F. H. (2017, February 15-16). *Synthesis of reduced Graphene Oxide (rGO) using different treatments of Graphene Oxide (GO)*. [Paper presentation]. IOP Conference Series: Materials Science and Engineering, Putrajaya, Malaysia. <https://doi.org/10.1088/1757-899X/358/1/012046>

